

Differentially Private Optimal Power Flow for Distribution Grids

Vladimir Dvorkin Jr., *Student member, IEEE*, Ferdinando Fioretto, Pascal Van Hentenryck, *Member, IEEE*, Jalal Kazempour, *Senior Member, IEEE*, and Pierre Pinson, *Fellow, IEEE*

Abstract—Although distribution grid customers are obliged to share their consumption data with distribution system operators (DSOs), a possible leakage of this data is often disregarded in operational routines of DSOs. This paper introduces a privacy-preserving optimal power flow (OPF) mechanism for distribution grids that secures customer privacy from unauthorised access to OPF solutions, e.g., current and voltage measurements. The mechanism is based on the framework of *differential privacy* that allows to control the participation risks of individuals in a dataset by applying a carefully calibrated noise to the output of a computation. Unlike existing private mechanisms, this mechanism does not apply the noise to the optimization parameters or its result. Instead, it optimizes OPF variables as affine functions of the random noise, which weakens the correlation between the grid loads and OPF variables. To ensure feasibility of the randomized OPF solution, the mechanism makes use of chance constraints enforced on the grid limits. The mechanism is further extended to control the optimality loss induced by the random noise, as well as the variance of OPF variables. The paper shows that the differentially private OPF solution does not leak customer loads up to specified parameters.

Index Terms—Data obfuscation, optimization methods, privacy

I. INTRODUCTION

THE increasing observability of distribution grids enables advanced operational practices for distribution system operators (DSOs). In particular, high-resolution voltage and current measurements available to DSOs allow for continuously steering the system operation towards an optimal power flow (OPF) solution [1]–[3]. However, when collected, these measurements expose distribution grid customers to privacy breaches. Several studies have shown that the measurements of OPF variables can be used by an adversary to identify the type of appliances and load patterns of grid customers [4], [5]. The public response to these privacy risks has been demonstrated by the Dutch Parliament’s decision to thwart the deployment of smart meters until the privacy concerns are resolved [6].

Although grid customers tend to entrust DSOs with their data in exchange for a reliable supply, their privacy rights are often disregarded in operational routines of DSOs. To resolve this issue, this paper augments the OPF computations with the preservation of customer privacy in the following sense.

Definition 1 (Customer privacy). *The right of grid customers to be secured from an unauthorized disclosure of sensitive information that can be inferred from the OPF solution.*

V. Dvorkin Jr., J. Kazempour, and P. Pinson are with the Technical University of Denmark, Kgs. Lyngby, Denmark. F. Fioretto is with the Syracuse University, Syracuse, NY, USA. P. Van Hentenryck is with the Georgia Institute of Technology, Atlanta, GA, USA.

To ensure this right, privacy needs to be rigorously quantified and guaranteed. Differential privacy (DP) [7] is a strong privacy notion that quantifies and bounds privacy risks in computations involving sensitive datasets. By augmenting the computations with a carefully calibrated *random* noise, a DP *mechanism* guarantees that the noisy results do not disclose the attributes of individual items in a dataset. Chaudhuri *et al.* [8] and Hsu *et al.* [9] introduced several mechanisms to solve optimization models while preventing the recovery of the input data from optimization results. These mechanisms apply noise to either the parameters or the results of an optimization. The applied noise, however, fundamentally alters the optimization problem of interest. Therefore, the direct application of these mechanisms to OPF problems has been limited. First, they may fail to provide a *feasible* solution for constrained optimization problems. To restore feasibility, they require an additional level of complexity such as the post-processing steps proposed in [10], [11]. Second, although these mechanisms provide bounds on the worst-case performance, they do not consider the *optimality loss* as a control variable. As a result, they cannot provide appropriate trade-offs between the expected and the worst-case mechanism performances. Finally, the previously proposed mechanisms overlook the impact of the noise on the *variance* of the optimization results. Hence, their direct application to OPF problems may lead to undesired overloads of system components [12].

Contributions: To overcome these limitations, this paper proposes a novel differentially private OPF mechanism that does not add the noise to the optimization parameters or to the results. Instead, it obtains DP by optimizing OPF variables as *affine functions* of the noise, bypassing the above-mentioned theoretical drawbacks. More precisely, the paper makes the following contributions:

1. The proposed mechanism produces a random OPF solution that follows a Normal distribution and guarantees (ϵ, δ) -differential privacy [7]. The parameters ϵ and δ , respectively, bound the multiplicative and additive differences between the probability distributions of OPF solutions obtained on adjacent datasets (i.e., differing in at most one load value). The mechanism is particularly suitable for protecting grid loads from unauthorized access to OPF solutions, as fine-tuned (ϵ, δ) values make randomized OPF solutions similar, irrespective of the used load dataset.
2. The mechanism enforces chance constraints on random OPF variables to guarantee solution feasibility for a given constraint satisfaction probability. This way, it does not require a post-processing step to restore OPF feasibility, as in [10] and [11]. Since the OPF variables are affine in the

Gaussian noise, the chance constraints are reformulated into computationally efficient second-order cone constraints.

3. The mechanism enables the control of random OPF outcomes without weakening the DP guarantees. Using results from stochastic programming [13], the optimality loss induced by the noise is controlled using Conditional Value-at-Risk (CVaR) risk measure, enabling the trade-off between the expected and the worst-case performance. Furthermore, with a variance-aware control from [14], the mechanism attains DP with a smaller variance of OPF variables.

Related Work: Thanks to its strong privacy guarantees, DP has been recently applied to private OPF computations. In particular, the mechanism of Zhou *et al.* [15] releases aggregated OPF statistics, e.g., aggregated load, while ensuring the privacy for individual loads, even if all but one loads are compromised. The proposals by Fioretto *et al.* [10] and Mak *et al.* [11] provide a differentially private mechanism to release high-fidelity OPF datasets (e.g., load and network parameters) from real power systems while minimizing the risks of disclosing the actual system parameters. The mechanisms, however, are meant for the private release of aggregate statistics and input datasets and do not provide the OPF solution itself.

Private OPF computations have also been studied in a decentralized setting. Dvorkin *et al.* [16] designed a distributed OPF algorithm with a differentially private exchange of coordination signals, hence preventing the leakage of sensitive information in the algorithm subproblems. Han *et al.* [17] proposed a privacy-aware distributed coordination scheme for electrical vehicle charging. The privacy frameworks in [16] and [17], however, are not suitable for centralized computations. In distribution systems, Zhang *et al.* [18], among other proposals reviewed in [6], designed a privacy-aware optimization of behind-the-meter energy storage systems to prevent the leakage of consumption data from the smart meter readings. However, they disregard OPF feasibility of distribution systems, which has to be preserved in all circumstances.

Paper Organization: Following the preliminaries in Section II, Section III formalizes the privacy goals and provides an overview of the proposed solution. Section IV provides the formulation of the proposed privacy-preserving OPF mechanism, whereas Section V presents its properties and extensions. Finally, Section VI provides numerical experiments.

II. PRELIMINARIES

A. Optimal Power Flow Problem

The paper considers a low-voltage radial distribution grid with controllable distributed energy resources (DERs). A DSO is responsible for controlling the DERs and supplying power from the high-voltage grid while meeting the technical limits of the grid. The grid is modeled as a graph $\Gamma(\mathcal{N}, \mathcal{L})$, where $\mathcal{N} = \{0, 1, \dots, n\}$ is the set of nodes and $\mathcal{L} = \mathcal{N} \setminus \{0\}$ is the set of lines connecting those nodes. The root node, indexed by 0, is a substation with a large capacity and fixed voltage magnitude $v_0 = 1$. The radial topology, depicted in Fig. 1, associates each node $i \in \mathcal{N}$ with the sets \mathcal{U}_i and \mathcal{D}_i of, respectively, upstream and downstream nodes, as well as with the set \mathcal{R}_i of nodes on the path to the root node.

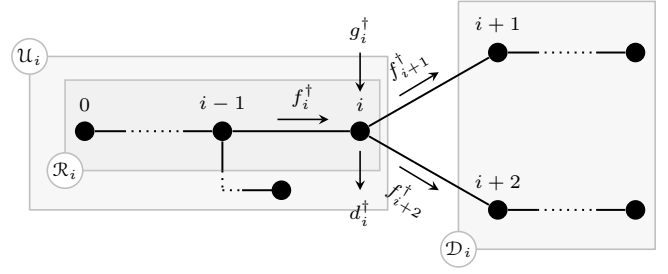


Fig. 1. Topology of the distribution grid relative to node i , $\dagger = \{p, q\}$.

Each node i is characterized by its fixed active d_i^p and reactive d_i^q power load and by its voltage magnitude $v_i \in [\underline{v}_i, \bar{v}_i]$. For modeling convenience, the voltage variables are substituted by $u_i = v_i^2$, $\forall i \in \mathcal{N}$. A controllable DER sited at node i outputs an amount of active $g_i^p \in [\underline{g}_i^p, \bar{g}_i^p]$ and reactive $g_i^q \in [\underline{g}_i^q, \bar{g}_i^q]$ power. Its costs are linear with a cost coefficient c_i . To model the relation between active and reactive power output, the paper assumes a constant power factor $\tan \phi_i$. Similarly, the constant power factor is assumed for loads, such that each load i can be described solely by its active component d_i^p . The active and reactive power flows, f_ℓ^p and f_ℓ^q , $\forall \ell \in \mathcal{L}$, respectively, are constrained by the apparent power limit \bar{f}_ℓ , and each line is characterized by its resistance r_ℓ and reactance x_ℓ . The deterministic OPF model is formulated as:

$$\text{D-OPF: } \min_{g^\dagger, f^\dagger, u} \sum_{i \in \mathcal{N}} c_i g_i^\dagger \quad (1a)$$

$$\text{s.t. } g_0^\dagger = \sum_{i \in \mathcal{D}_0} (d_i^\dagger - g_i^\dagger), u_0 = 1, \quad (1b)$$

$$f_\ell^\dagger = d_\ell^\dagger - g_\ell^\dagger + \sum_{i \in \mathcal{D}_\ell} (d_i^\dagger - g_i^\dagger), \forall \ell \in \mathcal{L}, \quad (1c)$$

$$u_i = u_0 - 2 \sum_{\ell \in \mathcal{R}_i} (f_\ell^p r_\ell + f_\ell^q x_\ell), \forall i \in \mathcal{N} \setminus \{0\}, \quad (1d)$$

$$(f_\ell^p)^2 + (f_\ell^q)^2 \leq \bar{f}_\ell^2, \forall \ell \in \mathcal{L}, \quad (1e)$$

$$\underline{g}_i^\dagger \leq g_i^\dagger \leq \bar{g}_i^\dagger, \forall i \in \mathcal{N}, \quad (1f)$$

$$\underline{v}_i^2 \leq u_i \leq \bar{v}_i^2, \forall i \in \mathcal{N} \setminus \{0\}, \quad (1g)$$

where superscript $\dagger = \{p, q\}$ indexes active and reactive power. The objective is to minimize the total operational cost subject to the OPF equations (1b)–(1d) and grid limits (1e)–(1g). The OPF equations balance the grid based on the *LinDistFlow* AC power flow equations [19].

B. Differential Privacy

The paper uses the framework of *differential privacy* [7] to quantify and control the privacy risks of the customer loads. It considers datasets $D \in \mathbb{R}^n$ as n -dimensional vectors describing the *active* load values, denoted by d_i for each node i . To protect the participation of the load in the i^{th} entry of the dataset, the following *adjacency relation* is introduced:

$$D \sim_\beta D' \Leftrightarrow \exists i \text{ s.t. } |d_i - d'_i| \leq \beta_i \wedge d_j = d'_j, \forall j \neq i,$$

where D and D' are two adjacent datasets, $\beta \in \mathbb{R}^n$ is a vector of positive real values, and the values d_i and d'_i are the load values corresponding to customer i in D and D' , respectively.

The adjacency relation relates two load vectors that differ in at most one item, at position i , by a value not greater than β_i .

If a mechanism satisfies the definition of differential privacy, it returns similar results on adjacent datasets in a probabilistic sense. This intuition is formalized in the following definition.

Definition 2 (Differential Privacy). *Given a value $\beta \in \mathbb{R}_+^n$, a randomized mechanism $\tilde{\mathcal{M}}: \mathcal{D} \rightarrow \mathcal{R}$ with domain \mathcal{D} and range \mathcal{R} is (ε, δ) -differential private if, for any output $s \subseteq \mathcal{R}$ and any two adjacent inputs $D \sim_\beta D' \in \mathbb{R}^n$*

$$\mathbb{P}[\tilde{\mathcal{M}}(D) \in s] \leq e^\varepsilon \mathbb{P}[\tilde{\mathcal{M}}(D') \in s] + \delta,$$

where \mathbb{P} denotes the probability over runs of $\tilde{\mathcal{M}}$.

The level of privacy is controlled by DP parameters (ε, δ) . The former corresponds to the maximal multiplicative difference in distributions obtained by the mechanism on adjacent datasets, whereas the latter defines the maximal additive difference. Consequently, smaller values of ε and δ provide stronger privacy protection. Definition 2 extends the metric-based differential privacy introduced by Chatzikokolakis *et al.* [20] to control of *individual* privacy risks.

The differentially private design of any mechanism is obtained by means of randomization using, among others, Laplace, Gaussian, or exponential noise [21]. The DP requirements for an optimization problem are achieved by introducing a calibrated noise to the input data [9] or to the output or objective function of the mechanism itself [8]. Regardless of the strategy adopted to attain DP, the amount of noise to inject depends on the mechanism *sensitivity*. In particular, the L_2 -sensitivity of a deterministic mechanism \mathcal{M} on β -adjacent datasets, denoted by Δ^β , is defined as:

$$\Delta^\beta = \max_{D \sim_\beta D'} \|\mathcal{M}(D) - \mathcal{M}(D')\|_2.$$

This work makes use of the Gaussian mechanism, which provides (ε, δ) -differential privacy as per the following result.

Theorem 1 (Gaussian mechanism [21]). Let \mathcal{M} be a mechanism of interest that maps datasets D to \mathbb{R}^n . For $\varepsilon \in (0, 1)$ and $\gamma^2 > 2 \ln(\frac{1.25}{\delta})$, the Gaussian mechanism that outputs $\tilde{\mathcal{M}}(D) = \mathcal{M}(D) + \xi$, with ξ noise drawn from the Normal distribution with 0 mean and standard deviation $\sigma \geq \gamma \frac{\Delta^\beta}{\varepsilon}$ is (ε, δ) -differentially private.

When the DP mechanism produces solutions to an optimization problem, it is also important to quantify the *optimality loss*, i.e., the distance between the optimal solutions of the original mechanism $\mathcal{M}(D)$ and its differentially private counterpart $\tilde{\mathcal{M}}(D)$ evaluated on the original dataset D .

III. PROBLEM STATEMENT

In the context of the underlying dispatch problem, the DSO collects a dataset $D = \{d_i^p\}_{i \in \mathcal{N}}$ of customer *sensitive* loads and dispatches the DER according to the solution of the OPF model (1). The OPF model acts as a mechanism $\mathcal{M}: D \mapsto s$ that maps the dataset D into an optimal OPF solution s^* . The solution is a tuple comprising generator set points $\{g_i^p, g_i^q\}_{i \in \mathcal{N}}$, power flows $\{f_\ell^p, f_\ell^q\}_{\ell \in \mathcal{L}}$, and voltages $\{u_i\}_{i \in \mathcal{N}}$, as depicted on the left plane in Fig. 2. However, the release of s^* poses

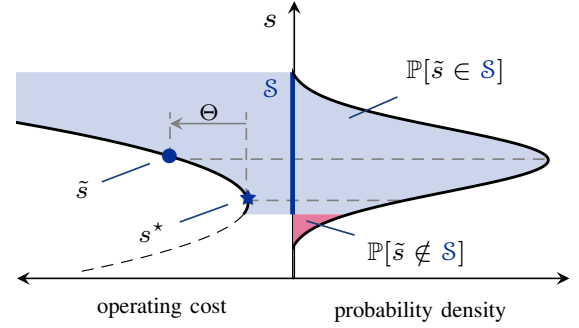


Fig. 2. Projections of OPF solutions onto operating cost and feasibility space.

a privacy threat: an adversary with access to the items in s^* could *decode* the customers activities [4], [5]. For instance, the voltage sags at a node of interest discloses the activity of residential costumers (e.g., charging an electrical vehicle). Voltages and flows (currents) also encode information about the technology, production patterns, and other commercial data of industrial customers [10].

To minimize privacy risks, this work proposes a mechanism $\tilde{\mathcal{M}}$ for the DSO, which returns a feasible solution \tilde{s} at the expense of an optimality loss, as shown in Fig. 2. A non-trivial benefit of choosing \tilde{s} over s^* is that the former includes a particular perturbation of the optimal solution and thus carries less information about the real load data D . For instance, the sub-optimal solution can feature a more intensive deployment of the DERs to compensate for the voltage sags instead of purchasing power from the high-voltage grid. To ensure that $\tilde{\mathcal{M}}$ returns a differentially private solution, \tilde{s} has to follow a carefully calibrated noise distribution, as depicted on the right plane in Fig. 2. In other words, the mechanism must satisfy Definition 2, i.e., on adjacent load datasets, it must output distributions (describing the generator outputs, flows, and voltages) that differ by at most ε and δ in multiplicative and additive terms, respectively. However, with smaller ε and δ , the variance of the OPF solutions and hence the probability of producing an infeasible solution increases. The mechanism thus needs to address this feasibility issue. Finally, the last desired property is the ability to control the induced optimality loss Θ in order to ensure cost-effective grid operations.

IV. DIFFERENTIALLY PRIVATE OPF MECHANISM

This section provides a mathematical description of mechanism $\tilde{\mathcal{M}}$ and details its application. The intuition behind the mechanism is as follows. Consider an optimal OPF solution s^* . The DP mechanism could perturb the optimal power flows in s^* with random noise ξ and then adapt the optimal generation schedule and voltages to match the perturbed power flows. However, there is no guarantee that this will result in a feasible dispatch. To remedy this limitation, the mechanism does not use s^* , but instead solves a chance-constrained optimization that produces an OPF solution \tilde{s}^* , which is robust to flow perturbations, i.e., with high probability, it is possible to find a feasible generator dispatch and its associated voltages for any calibrated noise injection on the power flow. Once \tilde{s}^* is obtained, the mechanism perturbs the power flows in \tilde{s}^*

and adapts the generation dispatch and voltage magnitudes, accordingly. Subsection IV-A describes how the noise on power flows is generated and how the generator dispatch and voltages can be modified to accommodate the noise, Subsection IV-B presents the chance-constrained optimization, and Subsection IV-C summarizes the mechanism.

A. Random Perturbation of OPF Solutions

To guarantee differential privacy, the proposed mechanism perturbs the OPF variables $\{g_i^\dagger\}_{i \in \mathcal{N}}$ and $\{f_i^\dagger, u_i\}_{i \in \mathcal{L}}$. Since the OPF equations (1b)–(1d) couple these variables, it suffices to perturb only one set of variables to induce a change in the overall solution. For instance, by perturbing the active power flow f_i^p , the reactive power flow f_i^q , voltage magnitude u_i , and DER output g_i^\dagger associated with node i , need to be adjusted accordingly. *The perturbation of power flows is particularly convenient, as their sensitivity to loads can be directly upper-bounded by the load magnitudes in radial grids.*

The proposed mechanism perturbs the active power flows by a random variable $\xi \in \mathbb{R}^{|\mathcal{L}|}$ that obeys a Normal distribution $\mathcal{N}(0, \Sigma)$ with covariance matrix

$$\Sigma = \text{diag}([\sigma_1^2, \dots, \sigma_{|\mathcal{L}|}^2]) = \text{diag}(\sigma^2) \in \mathbb{R}^{|\mathcal{L}| \times |\mathcal{L}|}.$$

The paper refers to Σ , σ^2 , and σ interchangeably to discuss the perturbation parameters. To accommodate this perturbation, the mechanism imposes the following affine policies:

$$\tilde{g}_i^p = g_i^p + \sum_{\ell \in \mathcal{D}_i} \alpha_{i\ell} \xi_\ell - \sum_{\ell \in \mathcal{U}_i} \alpha_{i\ell} \xi_\ell, \quad \forall i \in \mathcal{N}, \quad (2a)$$

where \tilde{g}_i^p and g_i^p are, respectively, the random and nominal DER active power outputs, and $\alpha_{i\ell}$ is the portion of random perturbation ξ_ℓ accommodated by the DER at node i , modeled as a free variable. To make policy (2a) viable, the following balancing conditions are enforced:

$$\sum_{i \in \mathcal{U}_\ell} \alpha_{i\ell} = 1, \quad \sum_{i \in \mathcal{D}_\ell} \alpha_{i\ell} = 1, \quad \forall \ell \in \mathcal{L}, \quad (2b)$$

such that the perturbation of flow f_ℓ^p causes the upstream DERs to adjust their aggregated output by ξ_ℓ and the downstream DERs to counterbalance this perturbation by ξ_ℓ .

To provide a succinct representation of the randomized OPF variables, consider a topology matrix $T \in \mathbb{R}^{|\mathcal{N}| \times |\mathcal{L}|}$ whose elements are such that:

$$T_{i\ell} = \begin{cases} 1, & \text{if line } \ell \text{ is downstream w.r.t. node } i, \\ -1, & \text{if line } \ell \text{ is upstream w.r.t. node } i \\ 0, & \text{otherwise.} \end{cases}$$

Consider also an auxiliary row vector $\rho_i^p = T_i \circ \alpha_i$ that returns a Schur product of i^{th} row of T and i^{th} row of α , and set $\rho_i^q = \rho_i^p \tan \phi_i$. Using this notation, the perturbed OPF solution is modeled as the following set of random variables:

$$\tilde{g}_i^\dagger = g_i^\dagger + \rho_i^\dagger \xi, \quad \forall i \in \mathcal{N}, \quad (3a)$$

$$\tilde{f}_\ell^\dagger = f_\ell^\dagger - \left[\rho_\ell^\dagger + \sum_{j \in \mathcal{D}_\ell} \rho_j^\dagger \right] \xi, \quad \forall \ell \in \mathcal{L}, \quad (3b)$$

$$\tilde{u}_i = u_i + 2 \sum_{j \in \mathcal{R}_i} \left[r_j (\rho_j^p + \sum_{k \in \mathcal{D}_j} \rho_k^p) + x_j (\rho_j^q + \sum_{k \in \mathcal{D}_j} \rho_k^q) \right] \xi, \quad \forall i \in \mathcal{L}, \quad (3c)$$

where the randomized power flows \tilde{f}_i^\dagger are obtained by substituting generator policy (2a) into (1c), and randomized voltage magnitudes \tilde{u}_i are expressed by substituting \tilde{f}_i^\dagger into (1d). Each variable is thus represented by its nominal component and its random component whose realization depends on ξ . By properly calibrating the parameters of ξ , the randomized OPF solution in (3) provides the required differential privacy guarantees for grid customers (see Section V, Theorem 2). However, there is no guarantee that the randomized OPF solution in (3) is feasible.

B. The Chance-Constrained Optimization Problem

To obtain a feasible dispatch, the proposed mechanism uses a chance-constrained optimization whose optimal solution, when carefully perturbed, will be feasible with high probability. The chance-constrained program is obtained by substituting variables (3) into the base OPF model (1) and enforcing chance constraints on the grid limits. The tractable formulation of the chance-constrained program is provided in (4), which is obtained considering the following transformations.

1) *Objective Function Reformulation:* The chance-constrained program minimizes the *expected* cost, which is reformulated as follows:

$$\mathbb{E}_\xi \left[\sum_{i \in \mathcal{N}} c_i \tilde{g}_i^p \right] = \mathbb{E}_\xi \left[\sum_{i \in \mathcal{N}} c_i (g_i^\dagger + \rho_i^\dagger \xi) \right] = \sum_{i \in \mathcal{N}} c_i g_i^p, \quad \forall i \in \mathcal{N},$$

due to the zero-mean distribution of ξ .

2) *Approximation of the Quadratic Power Flow Constraints:* The substitution of the random power flow variables in (3b) into the apparent power flow limit constraints (1e) results in the following expression

$$(\tilde{f}_\ell^p)^2 + (\tilde{f}_\ell^q)^2 \leq \bar{f}_\ell^2, \quad \forall \ell \in \mathcal{L},$$

which exhibits a quadratic dependency on random variable ξ , for which no tractable chance-constrained reformulation is known. To resolve this issue, the above quadratic constraint is replaced by the inner polygon [22], [23], which writes as

$$\gamma_c^p \tilde{f}_i^p + \gamma_c^q \tilde{f}_i^q + \gamma_c^s \bar{f}_i \leq 0, \quad \forall i \in \mathcal{L}, \forall c \in \mathcal{C},$$

where γ_c^p, γ_c^q , and γ_c^s are the coefficients for each side c of the polygon. The cardinality $|\mathcal{C}|$ is arbitrary, but a higher cardinality brings a better accuracy.

3) *Conic Reformulation of Linear Chance Constraints:* For the normally distributed random variable ξ , the chance constraint of the form $\mathbb{P}_\xi[\xi^\top x \leq b] \geq 1 - \eta$ is translated into a second-order cone constraint as [24, Chapter 4.2.2]:

$$z_\eta \|\text{Std}(\xi^\top x)\|_2 \leq b - \mathbb{E}_\xi[\xi^\top x],$$

where $z_\eta = \Phi^{-1}(1 - \eta)$ is the inverse cumulative distribution function of the standard Gaussian distribution at the $(1 - \eta)$ quantile, and η is the constraint violation probability. Therefore, the individual chance constraints on the generation, voltage, and power flow variables are formulated in a conic form in (4c)–(4g), respectively. The resulting tractable formulation of the chance-constrained OPF program is as follows:

$$\text{CC-OPF:} \quad \min_{\mathcal{V} = \{g^\dagger, f^\dagger, u, \rho^\dagger\}} \sum_{i \in \mathcal{N}} c_i g_i^p \quad (4a)$$

s.t. Equations (1b) – (1d), (2b), (4b)

$$z_{\eta^g} \|\rho_i^\dagger \sigma\|_2 \leq \bar{g}_i^\dagger - g_i^\dagger, \forall i \in \mathcal{N}, \quad (4c)$$

$$z_{\eta^g} \|\rho_i^\dagger \sigma\|_2 \leq \underline{g}_i^\dagger - \underline{g}_i^\dagger, \forall i \in \mathcal{N}, \quad (4d)$$

$$z_{\eta^u} \left\| \left[\sum_{j \in \mathcal{R}_i} [r_j (\rho_j^p + \sum_{k \in \mathcal{D}_j} \rho_k^p) + x_j (\rho_j^q + \sum_{k \in \mathcal{D}_j} \rho_k^q)] \right] \sigma \right\|_2 \leq \frac{1}{2} (\bar{u}_i - u_i), \forall i \in \mathcal{L}, \quad (4e)$$

$$z_{\eta^u} \left\| \left[\sum_{j \in \mathcal{R}_i} [r_j (\rho_j^p + \sum_{k \in \mathcal{D}_j} \rho_k^p) + x_j (\rho_j^q + \sum_{k \in \mathcal{D}_j} \rho_k^q)] \right] \sigma \right\|_2 \leq \frac{1}{2} (u_i - \underline{u}_i), \forall i \in \mathcal{L}, \quad (4f)$$

$$z_{\eta^f} \left\| \left(\gamma_c^p [\rho_\ell^p + \sum_{i \in \mathcal{D}_\ell} \rho_i^p] + \gamma_c^q [\rho_\ell^q + \sum_{i \in \mathcal{D}_\ell} \rho_i^q] \right) \sigma \right\|_2 \leq -\gamma_c^p f_\ell^p - \gamma_c^q f_\ell^q - \gamma_c^s \bar{f}_\ell, \forall \ell \in \mathcal{L}, \forall c \in \mathcal{C}. \quad (4g)$$

C. The Privacy-Preserving Mechanism

The privacy-preserving mechanism $\tilde{\mathcal{M}}$ is depicted in Fig. 3. The first step defines the covariance matrix Σ that encodes the DP parameters (ε, δ) , and adjacency parameter β . The mechanism then solves the optimization problem in (4) to obtain an optimal solution \hat{v} which will be feasible for any realization of $\xi \sim \mathcal{N}(0, \Sigma)$ up to some given constraint violation probabilities. In the last step, the mechanism samples ξ and obtains the final OPF solution using Equations (3).

V. MECHANISM PROPERTIES AND EXTENSIONS

This section reviews the properties of the privacy mechanism and some extensions.

A. Feasibility and Privacy Guarantees

The OPF variables in (3) can be viewed as probability density functions parameterized by ξ . The DSO obtains an OPF solution by sampling random variable ξ . *By design*, the sampled solution is guaranteed to satisfy grid limits and customer loads up to specified violation probabilities η^g, η^u and η^f , of the generator, voltage, and power flow constraints.

The privacy guarantees, in turn, depend on the specification of DP parameters (ε, δ) and the vector of adjacency coefficients β . For simplicity, the DP parameters are assumed to be uniform for all customers and specified by the DSO, whereas customer privacy preferences are expressed in the submitted adjacency coefficients. In this setting, the load of every customer i is guaranteed to be indistinguishable from any other load in the range $[d_i^p - \beta_i, d_i^p + \beta_i]$ in the release of OPF solution related to node i up to DP parameters (ε, δ) . This guarantee is formalized by the following result.

Theorem 2 (Privacy Guarantees). *Let $(\varepsilon, \delta) \in (0, 1)$ and $\sigma_i \geq \beta_i \sqrt{2 \ln(1.25/\delta)}/\varepsilon, \forall i \in \mathcal{L}$. Then, if problem (4) returns an optimal solution, mechanism $\tilde{\mathcal{M}}$ is (ε, δ) -differentially private for β -adjacent load datasets. That is, the probabilities of returning a power flow solution in set F^p on any two β -adjacent datasets D and D' are such that*

$$\mathbb{P}[\tilde{\mathcal{M}}(D) \in F^p] \leq e^\varepsilon \mathbb{P}[\tilde{\mathcal{M}}(D') \in F^p] + \delta,$$

where \mathbb{P} denotes the probability over runs of $\tilde{\mathcal{M}}$.

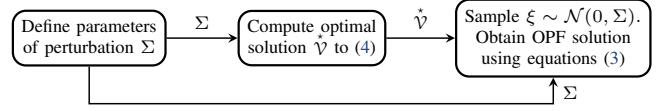


Fig. 3. The privacy-preserving mechanism $\tilde{\mathcal{M}}$.

Proof. The proof relies on two intermediate results summarized in Lemmas 1 and 2 in the appendix. The first lemma shows that the standard deviation of power flow related to customer i is at least as much as σ_i . Therefore, by specifying σ_i , the DSO attains the desired degree of randomization. The second lemma shows that $\beta_i \geq \Delta_i^\beta$, i.e., if σ_i is parameterized by β_i , then σ_i is also parameterized by sensitivity Δ_i^β , required by the Gaussian mechanism in Theorem 1. The full proof is available in an online Appendix [25]. \square

B. OPF Variance Control

Due to the radial topology of distribution grids, the flow perturbations along the same radial branch induce larger flow variances than those intended by the covariance matrix Σ . This section extends the mechanism $\tilde{\mathcal{M}}$ to reduce the overall flow variance while still preserving privacy guarantees. Two strategies are analyzed to achieve this goal.

1) *Total Variance Minimization:* The flow standard deviation, obtained from (3b), depends on the DER participation variables ρ^\dagger . Therefore, the variance of power flows can be controlled by optimizing the DER dispatch. This variance control strategy is enabled by replacing problem (4) at the core of mechanism $\tilde{\mathcal{M}}$ by the following optimization:

$$\text{ToV-CC-OPF: } \min_{\forall \cup \{t\}} \sum_{i \in \mathcal{N}} c_i g_i^p + \sum_{\ell \in \mathcal{L}} \psi_\ell t_\ell \quad (5a)$$

$$\text{s.t. } \left\| [\rho_\ell^p + \sum_{i \in \mathcal{D}_\ell} \rho_i^p] \sigma \right\|_2 \leq t_\ell, \forall \ell \in \mathcal{L}, \quad (5b)$$

$$\text{Equations (4b) – (4g),} \quad (5c)$$

where the decision variable t_ℓ represents the standard deviation of the active power flow in line ℓ , which is penalized in the objective function by a non-negative parameter ψ_ℓ . By choosing $\psi_\ell, \forall \ell \in \mathcal{L}$, the DSO minimizes the total variance at the expense of operational cost. Note that, by Lemma 1, optimization (5) does not violate the privacy guarantees.

2) *Pursuing Target Variance:* This strategy solely perturbs the flow in the selected line of the radial branch (e.g., adjacent to the customer with the strongest privacy requirement) and constrains the DERs to maintain the flow variance in each line as required by the original matrix Σ . It specifies a new matrix $\hat{\Sigma} = \text{diag}([\hat{\sigma}_1^2, \dots, \hat{\sigma}_{|\mathcal{L}|}^2])$, $\mathbb{1}^\top \hat{\sigma}^2 \leq \mathbb{1}^\top \sigma^2$, that contains a smaller number of perturbations. This control is enabled by replacing problem (4) by the following optimization:

$$\text{TaV-CC-OPF: } \min_{\forall \cup \{t, \tau\}} \sum_{i \in \mathcal{N}} c_i g_i^p + \sum_{\ell \in \mathcal{L}} \psi_\ell \tau_\ell \quad (6a)$$

$$\text{s.t. } \left\| [\rho_\ell^p + \sum_{i \in \mathcal{D}_\ell} \rho_i^p] \hat{\sigma} \right\|_2 \leq t_\ell, \forall \ell \in \mathcal{L}, \quad (6b)$$

$$\|t_\ell - \sigma_\ell\|_2 \leq \tau_\ell, \forall \ell \in \mathcal{L}, \quad (6c)$$

$$\text{Equations (4b) – (4g) with } \hat{\sigma}, \quad (6d)$$

where, t_ℓ returns the resulting flow standard deviation, while constraint (6c) yields the distance τ_ℓ between the resulting standard deviation and original one $\sigma_\ell = \Sigma_{\ell,\ell}^{1/2}$ required to provide customer at node ℓ with differential privacy. By penalizing this distance in the objective function, the DSO attains privacy at a smaller amount of random perturbations. Note, as optimization (6) acts on covariance matrix $\hat{\Sigma}$ instead of Σ , the DSO needs to verify a posteriori that $t_\ell \geq \sigma_\ell, \forall \ell \in \mathcal{L}$.

C. Optimality Loss Control

The application of mechanism $\tilde{\mathcal{M}}$ necessarily leads to an optimality loss compared to the solution of non-private mechanism \mathcal{M} . This section slightly abuses the notation and denotes the cost of the non-private OPF solution and that of the proposed DP mechanism when evaluated on a dataset D by $\mathcal{M}(D)$ and $\tilde{\mathcal{M}}(D)$, respectively. The optimality loss Θ is measured in expectation as the L_2 distance, i.e.,

$$\mathbb{E}[\Theta] = \|\mathcal{M}(D) - \mathbb{E}[\tilde{\mathcal{M}}(D)]\|_2,$$

as $\mathcal{M}(D)$ always provides a deterministic solution. However, the worst-case realization of $\tilde{\mathcal{M}}(D)$ may significantly exceed the expected value and lead to a larger optimality loss. To this end, this section introduces the optimality loss control strategy using the Conditional Value-at-Risk (CVaR) measure [13].

Consider $\varrho\%$ of the worst-case realizations of the optimally loss. The expected value of these worst-case realizations can be modeled as a decision variable using the CVaR measure as

$$\text{CVaR}_\varrho := \mu_c + \sigma_c \phi(\Phi^{-1}(1 - \varrho)) / \varrho, \quad (7)$$

where μ_c and σ_c represent the expected value and standard deviation of operational cost while ϕ and $\Phi^{-1}(1 - \varrho)$ denote the probability density function and the inverse cumulative distribution function at the $(1 - \varrho)$ quantile of the standard Normal distribution. From Section (IV-B), it follows that

$$\mu_c := \mathbb{E}[c^\top \tilde{g}^p] = \mathbb{E}[c^\top (g^p + \rho\xi)] = c^\top g^p,$$

for zero-mean ξ , and the standard deviation finds as

$$\sigma_c := \text{Std}[c^\top (g^p + \rho\xi)] = \text{Std}[c^\top (\rho\xi)] = \|c^\top (\rho\sigma)\|_2,$$

providing a convex reformulation of the CVaR in (7). Therefore, for some trade-off parameter $\theta \in [0, 1]$, the DSO can trade off the mean and CVaR_ϱ of the optimality loss by substituting problem (4) at the core of mechanism $\tilde{\mathcal{M}}$ by the following optimization CVaR-CC-OPF:

$$\min_{\forall \cup \sigma_c} (1 - \theta)c^\top g^p + \theta [c^\top g^p + \sigma_c \phi(\Phi^{-1}(1 - \varrho)) / \varrho] \quad (8a)$$

$$\text{s.t.} \quad \|c^\top (\rho\sigma)\|_2 \leq \sigma_c, \quad (8b)$$

$$\text{Equations (4b) - (4g)}, \quad (8c)$$

where the standard deviation σ_c is modeled as a decision variable. Notice, the optimality loss control by means of (8) does not violate the privacy guarantees as per Lemma 1.

VI. NUMERICAL EXPERIMENTS

The experiments consider a modified 15-node radial grid from [26], which includes network parameters taken from [27], nodal loads as given in Table I, and nodal DERs with cost coefficients drawn from Normal distribution $c_i \sim \mathcal{N}(10, 2)$ \$/MWh, generation limits $g_i^p = 0$ MW, $g_i^g = 8$ MW, and power factor $\tan\phi_i = 0.5, \forall i \in \mathcal{N}$. The constraint violation probabilities are set as $\eta^g = 1\%$, $\eta^u = 2\%$ and $\eta^f = 10\%$. The DP parameters are set to $\varepsilon \rightarrow 1, \delta = 1/n = 0.071$ with n being a number of grid customers, while the adjacency parameters $\beta_i, \forall i \in \mathcal{L}$, vary across the experiments. All models are implemented in Julia using the JuMP package [28], and all data and codes are relegated to the e-companion [25].

A. Illustrative Example

Assume that the customer at node 7 has an atypical load pattern representing its production technology. Her pattern is obtained by multiplying the maximum load by $k(t)$, a multiplier with the following three periodic components:

$$k(t) = \max\left\{\sin\frac{5}{10^2}t, \frac{7}{10}\right\} + \frac{5}{10^2} \sin\frac{5}{10^2}t + \frac{25}{10^3} \sin\frac{75}{100}t$$

where t is the time step. The non-private OPF solution provided by the D-OPF model leaks the information about this pattern through the power flow f_7^p and voltage v_7 readings, as displayed on the left plots in Fig. 4. To obfuscate the load pattern in the OPF solution, the customer submits the privacy preference β_7 , which is accommodated by the DSO using the DP mechanism $\tilde{\mathcal{M}}$ in Fig. 3. Figure 4 shows that by setting $\beta_7 \rightarrow 0.07$ MW, the presence of the smallest periodic component is obfuscated through randomization, while the presence of the two remaining components is still distinguished. With an increasing β_7 , the mechanism further obfuscates the medium and largest periodic components.

B. Privacy Guarantees

To illustrate the privacy guarantees of Theorem 2, consider the same grid customer at node 7 with the load of 2.35 MW. For β_7 , consider two adjacent load datasets D' and D'' , containing $d_7^p = d_7^p - \beta_7$ and $d_7^{pp} = d_7^p + \beta_7$, respectively. The non-private OPF mechanism returns the following power flows

$$\mathcal{M}(D') = 2.05\text{MW}, \mathcal{M}(D) = 2.35\text{MW}, \mathcal{M}(D'') = 2.65\text{MW},$$

for $\beta_7 = 0.3$ MW, clearly distinguishing the differences in datasets through power flow readings. The differentially private mechanism $\tilde{\mathcal{M}}$ in Fig. 3, in turn, obfuscates the load value used in the computation. Figure 5 shows that the mechanism makes the OPF solutions on the three datasets similar in the probabilistic sense, thus providing privacy guarantees for the original load dataset D . The maximal difference between the distributions of power flow solutions is bounded by the parameters ε and δ . Observe that the larger specification $\delta = 0.75$ results in weaker guarantees, as the distributions slightly stand out from one another. On the other hand, $\delta = 0.07$ yields a larger noise magnitude overlapping the support of the three distributions. The OPF solution to be implemented is obtained from a single sample drawn from the blue distribution. By observing a sample, an adversary cannot infer information about the dataset it came from.

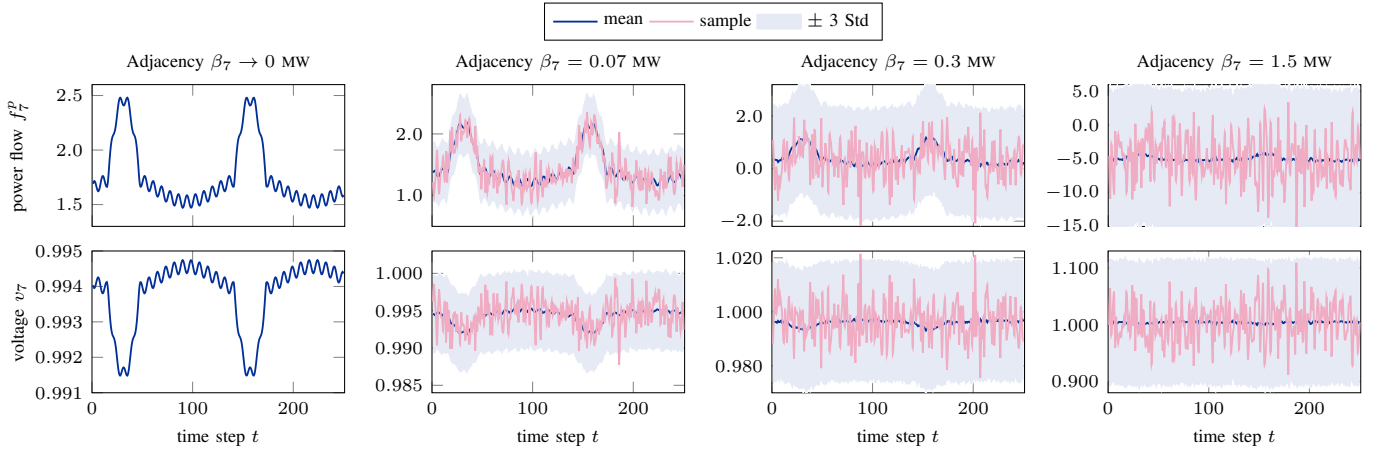


Fig. 4. Power flow and voltage magnitude at node 7 as functions of adjacency coefficient β_7 . The flow and voltage solutions are given by their mean value (blue) and the range of ± 3 standard deviations (light blue). The OPF solution implemented by the DSO is given by sample trajectories (red).

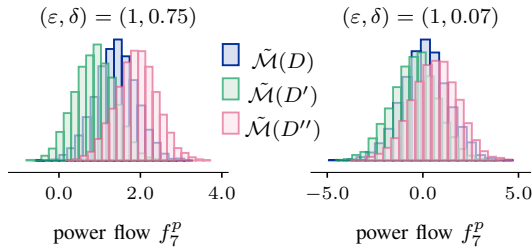


Fig. 5. The overlay of power flow probability densities obtained on the three β_7 -adjacent load datasets for $\delta = 0.75$ and $\delta = 0.07$.

C. OPF Variance Control

Consider the application of the mechanism when all grid customers have their adjacency coefficients set to 10% of their loads. The non-private D-OPF and private OPF solutions, obtained with the variance-agnostic CC-OPF and variance-aware ToV- and TaV-CC-OPF models, are summarized in Table I: Each row i presents the power flow and voltage solutions related to customer i , and the bottom rows report the expected operational cost, optimality loss $\mathbb{E}[\Theta]$ in %, sum of power flow standard deviations, percentage $\hat{\eta}$ of infeasible instances on 5000 noise samples, and CPU times.

The table shows that, unlike non-private, deterministic D-OPF model, the DP mechanisms return OPF variables as probability densities with given means and standard deviations. For all three DP mechanisms, the flow standard deviations are at least as much as those required by Theorem 2, thus providing differential privacy. However, due to the noise applied to each network flow, the flow standard deviations provided by the CC-OPF model exceed the intended quantities, e.g., by 458% for the first customer close to the substation. To minimize the OPF variance, the ToV-CC-OPF and TaV-CC-OPF models are used with the uniform variance penalty factor $\psi_\ell = 10^5, \forall \ell \in \mathcal{L}$. The ToV-CC-OPF model also perturbs each flow in the network but it alters the optimal DER dispatch to reduce the sum of flow standard deviations by 50%. The TaV-CC-OPF model, in turn, introduces a limited number of perturbations to lines $\{1, 5 - 7, 9, 11 - 13\}$ and constrains the DERs to maintain the intended standard deviation σ across the

entire network, reducing the flow standard deviation by 63%. As ToV-CC-OPF and TaV-CC-OPF prioritize the flow variance over expected cost, the models provide larger optimality loss than the CC-OPF model.

The OPF solution to be implemented by the DSO is a sample drawn from the probability densities reported in Table I. The empirical probability of the joint constraint violation $\hat{\eta}$ demonstrates an appropriate out-of-sample performance. However, if the DP mechanism returns an infeasible sample, the DSO may re-sample the OPF solution at the expense of a marginal relaxation of privacy guarantees. Finally, the privacy-preserving mechanisms keep the CPU time acceptable.

D. Optimality Loss Control

The DSO is capable to trade off between the expected and the worst-case optimality loss by substituting the CC-OPF model in mechanism $\tilde{\mathcal{M}}$ by the CVaR-CC-OPF model in (8). Consider the same setting as in the previous section. For a trade-off parameter $\theta \in [0, 1]$, the expected optimality loss in $\varrho = 10\%$ of the worst-case scenarios is contrasted with the expected loss in Table II. For $\theta = 0$, the CVaR_{10%} significantly exceeds the expected value. However, by increasing θ , the DSO alters the DER dispatch to reduce the worst-case optimality loss at the expense of increasing the expected value. For $\theta \geq 0.7$, the expected value corresponds to CVaR_{10%}, thus providing differential privacy at a fixed cost. Eventually, the choice of θ is driven by the DSO's risk preference.

VII. CONCLUSIONS

This paper introduced a differentially private OPF mechanism for distribution grids, which provides formal privacy guarantees for grid customer loads. The mechanism parametrizes OPF variables as affine functions of a carefully calibrated noise to weaken the correlations between grid loads and OPF variables, thus preventing the recovery of customer loads from the voltage and power flow measurements. Furthermore, the mechanism was extended to enable the DSO to control the OPF variance induced by the noise in the computations, providing better practices for systems with

TABLE I
SOLUTION SUMMARY FOR THE NON-PRIVATE AND DIFFERENTIALLY PRIVATE OPF MECHANISMS.

i	d_i^p	σ_i	D-OPF, Eq. (1)		CC-OPF, Eq. (4)				ToV-CC-OPF, Eq. (5)				TaV-CC-OPF, Eq. (6)			
			f_i^p	v_i	f_i^p		v_i		f_i^p		v_i		f_i^p		v_i	
					mean	std	mean	std	mean	std	mean	std	mean	std	mean	std
0	0	–	–	1.00	–	–	1.00	–	–	1.00	–	–	–	–	1.00	–
1	2.01	0.48	8.5	1.00	11.3	2.68	1.00	0.0016	12.6	0.69	1.00	0.0004	13.0	0.48	1.00	0.0003
2	2.01	0.48	6.5	1.00	9.3	2.68	0.99	0.0057	11.4	0.71	0.99	0.0015	11.0	0.48	0.99	0.0010
3	2.01	0.48	4.4	1.00	7.3	2.68	0.99	0.0123	10.2	0.78	0.97	0.0033	9.0	0.48	0.98	0.0022
4	1.73	0.41	-8.0	1.00	-1.4	1.72	0.99	0.0128	3.6	0.69	0.97	0.0034	1.7	0.41	0.98	0.0023
5	2.91	0.70	5.1	1.00	3.1	0.87	0.99	0.0128	2.5	0.82	0.97	0.0035	1.9	0.70	0.98	0.0024
6	2.19	0.52	2.2	1.00	0.1	0.87	0.99	0.0128	0.7	0.63	0.97	0.0038	1.0	0.52	0.98	0.0024
7	2.35	0.56	2.3	0.99	0.9	0.63	0.98	0.0134	0.9	0.61	0.97	0.0039	1.0	0.56	0.98	0.0024
8	2.35	0.56	10.5	0.99	6.7	1.18	0.98	0.0130	5.8	0.78	0.97	0.0036	6.4	0.56	0.98	0.0023
9	2.29	0.55	5.8	0.99	3.5	0.88	0.98	0.0132	3.1	0.70	0.97	0.0037	3.6	0.55	0.98	0.0023
10	2.17	0.52	3.5	0.99	1.2	0.88	0.98	0.0135	1.6	0.65	0.97	0.0038	1.3	0.52	0.97	0.0023
11	1.32	0.32	1.3	0.99	0.4	0.39	0.98	0.0135	0.4	0.40	0.97	0.0038	0.6	0.32	0.97	0.0023
12	2.01	0.48	6.5	1.00	3.6	1.23	1.00	0.0008	3.3	0.73	1.00	0.0004	3.6	0.48	1.00	0.0003
13	2.24	0.54	4.5	0.99	1.6	1.23	1.00	0.0034	2.1	0.72	1.00	0.0019	3.2	0.54	0.99	0.0012
14	2.24	0.54	2.2	0.99	-0.6	1.23	1.00	0.0050	0.8	0.64	0.99	0.0027	1.0	0.54	0.99	0.0018
cost ($\mathbb{E}[\Theta]$)			\$396.0 (0%)		\$428.0 (8.1%)				\$463.5 (17.1%)				\$459.3 (16.0%)			
$\sum_i \text{Std}[f_i^p]$			0 MW		19.1 MW				9.5 MW				7.1 MW			
infeas. $\hat{\eta}$			0%		3.3%				6.9%				5.5%			
CPU time			0.016s		0.037s				0.043s				0.052s			

TABLE II
TRADE-OFFS OF THE EXPECTED AND CVAR_{10%} PERFORMANCE

θ	exp. value		CVAR _{10%}		$\sum_i \text{Std}[f_i^p]$, MW
	cost, \$	Θ , %	cost, \$	Θ , %	
0.0	428.0	8.1	478.1	20.7	19.1
0.1	428.0	8.1	476.3	20.3	19.4
0.2	428.3	8.2	475.0	19.9	19.6
0.3	428.9	8.3	473.3	19.5	19.8
0.4	431.9	9.1	467.8	18.1	17.3
0.5	434.5	9.7	464.4	17.3	15.7
0.6	438.2	10.7	461.7	16.6	14.6
0.7	452.9	14.4	452.9	14.4	13.0

more emphasis on component overloads than on operational costs. Finally, the optimality loss induced by the mechanism translates into privacy costs. To minimize the risk of large privacy costs, the mechanism was extended to enable the trade-off between the expected and worst-case performances.

REFERENCES

- [1] E. Dall'Anese and A. Simonetto, "Optimal power flow pursuit," *IEEE Trans. Smart Grid*, vol. 9, no. 2, pp. 942–952, 2016.
- [2] S. Bolognani, E. Arcari, and F. Dörfler, "A fast method for real-time chance-constrained decision with application to power systems," *IEEE Contr. Syst. Lett.*, vol. 1, no. 1, pp. 152–157, 2017.
- [3] R. Mieth and Y. Dvorkin, "Data-driven distributionally robust optimal power flow for distribution systems," *IEEE Contr. Syst. Lett.*, vol. 2, no. 3, pp. 363–368, 2018.
- [4] C. Duarte *et al.*, "Non-intrusive load monitoring based on switching voltage transients and wavelet transforms," in *2012 Future of Instrumentation International Workshop Proceedings*. IEEE, 2012, pp. 1–4.
- [5] A. I. Cole and A. Albicki, "Data extraction for effective non-intrusive identification of residential power loads," in *IMTC/98 Conference Proceedings*, vol. 2. IEEE, 1998, pp. 812–815.
- [6] Z. Erkin *et al.*, "Privacy-preserving data aggregation in smart metering systems: An overview," *IEEE Signal Processing Magazine*, vol. 30, no. 2, pp. 75–86, 2013.
- [7] C. Dwork *et al.*, "Calibrating noise to sensitivity in private data analysis," in *Theory of Cryptography Conference*. Springer, 2006, pp. 265–284.
- [8] K. Chaudhuri, C. Monteleoni, and A. D. Sarwate, "Differentially private empirical risk minimization," *Journal of Machine Learning Research*, vol. 12, no. Mar, pp. 1069–1109, 2011.
- [9] J. Hsu *et al.*, "Privately solving linear programs," in *ICALP*. Springer, 2014, pp. 612–624.
- [10] F. Fioretto, T. W. Mak, and P. Van Hentenryck, "Differential privacy for power grid obfuscation," *IEEE Trans. Smart Grid*, 2020.
- [11] T. W. Mak *et al.*, "Privacy-preserving power system obfuscation: A bilevel optimization approach," *IEEE Trans. Power Syst.*, 2020.
- [12] S. S. Baghsorkhi and I. A. Hiskens, "Impact of wind power variability on sub-transmission networks," in *2012 IEEE Power and Energy Society General Meeting*. IEEE, 2012, pp. 1–7.
- [13] A. Shapiro, D. Dentcheva, and A. Ruszczyński, *Lectures on stochastic programming: modeling and theory*. SIAM, 2009.
- [14] D. Bienstock and A. Shukla, "Variance-aware optimal power flow: Addressing the tradeoff between cost, security, and variability," *IEEE Control Netw. Syst.*, vol. 6, no. 3, pp. 1185–1196, 2019.
- [15] F. Zhou, J. Anderson, and S. H. Low, "Differential privacy of aggregated DC optimal power flow data," *arXiv preprint arXiv:1903.11237*, 2019.
- [16] V. Dvorkin *et al.*, "Differentially private distributed optimal power flow," *arXiv preprint arXiv:1910.10136*, 2019.
- [17] S. Han, U. Topcu, and G. J. Pappas, "Differentially private distributed constrained optimization," *IEEE Trans. Autom. Control*, vol. 62, no. 1, pp. 50–64, 2016.
- [18] Z. Zhang *et al.*, "Cost-friendly differential privacy for smart meters: Exploiting the dual roles of the noise," *IEEE Trans. Smart Grid*, vol. 8, no. 2, pp. 619–626, March 2017.
- [19] K. Turitsyn *et al.*, "Local control of reactive power by distributed photovoltaic generators," in *2010 First IEEE International Conference on Smart Grid Communications*, 2010, pp. 79–84.
- [20] K. Chatzikokolakis *et al.*, "Broadening the scope of differential privacy using metrics," in *International Symposium on Privacy Enhancing Technologies Symposium*. Springer, 2013, pp. 82–102.
- [21] C. Dwork and A. Roth, "The algorithmic foundations of differential privacy," *Foundations and Trends® in Theoretical Computer Science*, vol. 9, no. 3–4, pp. 211–407, 2014.
- [22] T. Akbari and M. T. Bina, "Linear approximated formulation of AC optimal power flow using binary discretisation," *IET Generation, Transmission & Distribution*, vol. 10, no. 5, pp. 1117–1123, 2016.
- [23] R. Mieth and Y. Dvorkin, "Distribution electricity pricing under uncertainty," *arXiv preprint arXiv:1905.07526*, 2019.
- [24] S. Boyd and L. Vandenberghe, *Convex optimization*. Cambridge university press, 2004.
- [25] V. Dvorkin *et al.* Online Appendix to DP-CC-OPF. [Online]. Available: https://github.com/wdvorkin/DP_CC_OPF
- [26] A. Papavasiliou, "Analysis of distribution locational marginal prices," *IEEE Trans. Smart Grid*, vol. 9, no. 5, pp. 4872–4882, 2017.
- [27] R. Mieth and Y. Dvorkin. Code supplement - DLMPs under uncertainty. [Online]. Available: https://github.com/korpuskel91/DLMP_uncertainty_CodeSupplement
- [28] M. Lubin and I. Dunning, "Computing in operations research using julia," *INFORMS J Comput.*, vol. 27, no. 2, pp. 238–248, 2015.

APPENDIX

The proof of Theorem 2 relies on Lemmas 1 and 2. The first lemma shows that the standard deviation of power flow related to customer i is at least as much as σ_i . Therefore, by specifying σ_i , the DSO attains the desired degree of randomization.

Lemma 1. *If OPF mechanism (4) returns optimal solution, then σ_ℓ is the lower bound on $\text{Std}[\tilde{f}_\ell^p]$.*

Proof. Consider a single flow perturbation with $\xi_\ell \sim \mathcal{N}(0, \sigma_\ell^2)$ and $\xi_j = 0, \forall j \in \mathcal{L} \setminus \ell$. The standards deviation of active power flow (3b) in optimum finds as

$$\text{Std}\left[f_\ell^p - \left[\rho_\ell^p + \sum_{j \in \mathcal{D}_\ell} \rho_j^p\right] \xi\right] = \text{Std}\left[\left[\rho_\ell^p + \sum_{j \in \mathcal{D}_\ell} \rho_j^p\right] \xi\right] = \text{Std}\left[\sum_{j \in \mathcal{D}_\ell} \alpha_{j\ell} \xi_\ell\right] \stackrel{(2b)}{=} \text{Std}[\xi_\ell] = \sigma_\ell, \quad (9)$$

where the second to the last equality follows from balancing conditions (2b). As for any pair $(\ell, j) \in \mathcal{L}$ the covariance matrix returns $\Sigma_{\ell, j} = 0$, σ_ℓ is a lower bound on $\text{Std}[f_\ell^p]$ in the optimum for any additional perturbation in the network. \square

Remark 1. *The result of Lemma 1 holds independently from the choice of objective function and is solely driven by the feasibility conditions.*

The second lemma shows that $\beta_i \geq \Delta_i^\beta$, i.e., if σ_i is parameterized by β_i , then σ_i is also parameterized by sensitivity Δ_i^β .

Lemma 2. *Let D and D' be two adjacent datasets differing in at most one load d_i^p by at most $\beta_i > 0$. Then,*

$$\Delta_i^\beta = \max_{\ell \in \mathcal{L}} \|\mathcal{M}(D)|_{f_\ell^p} - \mathcal{M}(D')|_{f_\ell^p}\|_2 \leq \beta_i$$

where the notation $\mathcal{M}(\cdot)|_{f_\ell^p}$ denotes the value of the optimal active power flow on line ℓ returned by the computation $\mathcal{M}(\cdot)$.

Proof. Let f_ℓ^p be the optimal solution for the active power flow in line ℓ obtained on input dataset $D = (d_1^p, \dots, d_n^p)$. From OPF equation (1c), it can be written as

$$f_\ell^p = d_\ell^p - g_\ell^p + \sum_{i \in \mathcal{D}_\ell} (d_i^p - g_i^p),$$

which expresses the flow as a function of the downstream loads and the optimal DER dispatch. A change in the active load d_ℓ^p translates into a change of power flow as

$$\frac{\partial f_\ell^p}{\partial d_\ell^p} = \underbrace{\frac{\partial d_\ell^p}{\partial d_\ell^p}}_1 - \frac{\partial g_\ell^p}{\partial d_\ell^p} + \sum_{i \in \mathcal{D}_\ell} \left(\underbrace{\frac{\partial d_i^p}{\partial d_\ell^p}}_0 - \frac{\partial g_i^p}{\partial d_\ell^p} \right) = 1 - \frac{\partial g_\ell^p}{\partial d_\ell^p} - \sum_{i \in \mathcal{D}_\ell} \frac{\partial g_i^p}{\partial d_\ell^p}, \quad (10)$$

where the last two terms are always non-negative due to convexity of model (1). The value of (10) attains maximum when

$$g_k^p = \bar{g}_k^p \mapsto \frac{\partial g_k^p}{\partial d_\ell^p} = 0, \quad \forall k \in \{\ell\} \cup \mathcal{D}_\ell. \quad (11)$$

Therefore, by combining (10) with (11) we obtain the maximal change of power flows as

$$\frac{\partial f_\ell^p}{\partial d_\ell^p} = 1.$$

Since the dataset adjacency relation considers loads d_ℓ^p that differ by at most β_ℓ , it suffices to multiply the above by β_ℓ to attain the result. It finds similarly that for a β_i change of any load $i \in \mathcal{N}$, all network flows change by at most β_i . \square

Proof of Theorem 2. Consider a customer at non-root node i . Mechanism $\tilde{\mathcal{M}}$ induces a perturbation on the active power flow f_i^p by a random variable $\xi_i \sim \mathcal{N}(0, \sigma_i^2)$. The randomized active power flow \tilde{f}_i^p is then given as follows:

$$\tilde{f}_i^p = f_i^p - \left[\rho_i^p + \sum_{j \in \mathcal{D}_i} \rho_j^p\right] \xi$$

where \star denotes optimal solution for optimization variables. For privacy parameters (ε, δ) , the mechanism specifies

$$\sigma_i \geq \beta_i \sqrt{2 \ln(1.25/\delta)} / \varepsilon, \quad \forall i \in \mathcal{L}.$$

As per Lemma 1, we know that σ_i is the lower bound on the standard deviation of power flow f_ℓ^p . From Lemma 2 we also know that the sensitivity Δ_i^β of power flow in line i to load d_i^p is upper-bounded by β_i , so we have

$$\text{Std}[\tilde{f}_i^p] \geq \sigma_i \geq \Delta_i^\beta \sqrt{2 \ln(1.25/\delta)} / \varepsilon.$$

Since the randomized power flow follow is now given by a Normal distribution with the standard deviation $\text{Std}[\tilde{f}_i^p]$ as above, by Theorem 1, mechanism $\tilde{\mathcal{M}}$ satisfies (ε, δ) -differential privacy for each grid customer up to adjacency parameter β . \square